Epilepsia Open

SHORT RESEARCH ARTICLE

Advanced structural multimodal imaging of a patient with subcortical band heterotopia

*Lohith G. Kini, †Ilya M. Nasrallah, ‡Carlos Coto, ‡Lindsay C. Ferraro, and ‡Kathryn A. Davis

Epilepsia Open, 1(3-4):152–155, 2016
doi: 10.1002/epi4.12019

Lohith G. Kini is a doctoral candidate at the University of Pennsylvania.

Summary

Subcortical band heterotopia (SBH) is a disorder of neuronal migration most commonly due to mutations of the *Doublecortin* (*DCX*) gene. A range of phenotypes is seen, with most patients having some degree of epilepsy and intellectual disability. Advanced diffusion and structural magnetic resonance imaging (MRI) sequences may be useful in identifying heterotopias and dysplasias of different sizes in drug-resistant epilepsy. We describe a patient with SBH and drug-resistant epilepsy and investigate neurite density, neurite dispersion, and diffusion parameters as compared to a healthy control through the use of multiple advanced MRI modalities. Neurite density and dispersion in heterotopia was found to be more similar to white matter than to gray matter. Neurite density and dispersion maps obtained using diffusion imaging may be able to better characterize different subtypes of heterotopia.

KEY WORDS: Diffusion imaging, Malformations of cortical development, Band heterotopia, Neurite density.

Subcortical band heterotopia (SBH), also known as double cortex syndrome, is a rare disorder of neuronal migration characterized by bands of heterotopic gray matter just beneath the cortex.[1] It is a genetically and phenotypically heterogeneous disorder, and varying degrees of epilepsy and intellectual disability are the most common clinical manifestations. With advances in diffusion and perfusion imaging in magnetic resonance imaging (MRI), focal and diffuse forms of malformations of cortical development (MCDs), like SBH, are being increasingly recognized as heterogeneous malformations. Advanced structural, diffusion, and functional imaging sequences could produce maps of neurite density, dispersion, and functional activation that allow clinicians to further stratify such patients.

We present a case of SBH and drug-resistant epilepsy and discuss the findings of multiple imaging modalities, including neurite orientation dispersion and density imaging (NODDI). To the best of our knowledge, this is the first report of SBH using NODDI.

Patient details

A 23-year-old right-handed woman with drug-resistant epilepsy was admitted to our epilepsy monitoring unit for increased seizure frequency. She is a college student without academic difficulties, history of developmental delay, or subjective cognitive abnormality and is otherwise healthy. Family history was notable for a brother who died at delivery due to lissencephaly; otherwise, there was no family history of epilepsy or developmental delay. Overall, her neuropsychological profile is indicative of strength in the verbal domain with relative weakness in visual-spatial skills. Memory function is excellent, which is similar to previous studies of memory in patients with SBH.[2,3] Neurological examination was normal, and no other abnormalities were found on physical examination. Brain MRI revealed bilateral diffuse cerebral subcortical band heterotopia. Genetic testing via *Doublecortin* (*DCX*) sequencing was

Accepted August 15, 2016.

*Department of Bioengineering, University of Pennsylvania, Philadelphia, Pennsylvania, U.S.A.; †Departments of Radiology, and ‡Neurology, Hospital of the University of Pennsylvania, Philadelphia, Pennsylvania, U.S.A.

Address correspondence to Lohith G. Kini, Department of Bioengineering, University of Pennsylvania, 240 Skirkanich Hall, 210 S 33rd St, Philadelphia, PA 19104, U.S.A. E-mail: lkini@mail.med.upenn.edu

positive: pathogenic frameshift mutation identified (c.355_356del, p.Leu119Glyfs*15). Mutations in the *DCX* gene are thought to account for up to 80% of females with SBH.[4]

Her seizures began at the age of 6. She described two types of seizures: (1) an aura of dizziness and fatigue followed by staring, occurring approximately 1–2 times every month; (2) generalized tonic-clonic seizures occurring approximately once every year. Seizures were not controlled on a combination of lamotrigine and levetiracetam. Prior treatment with carbamazepine had been ineffective in controlling her seizures. She was started on lacosamide during admission. Interictal electroencephalogram (EEG) demonstrated: (1) 9-Hz posterior dominant rhythm; and (2) frequent 1- to 2-s bursts of bifrontal sharply contoured theta activity. She had seven complex partial seizures during admission. Electrographic seizures were preceded by an aura of nonspecific dizziness and fatigue without ictal EEG correlate followed by staring and unresponsiveness. Ictal EEG demonstrated diffuse bifrontally predominant rhythmic 6-Hz spike-and-wave epileptiform discharges that evolved in frequency to 3 Hz and increased in amplitude. There was no clear focal onset. Each seizure lasted approximately 30–60 s and was followed by postictal diffuse polymorphic delta slowing.

Materials and Methods

After discharge from the hospital and obtaining written informed consent from the patient, multiple MR imaging modalities were performed as a part of a research epilepsy imaging protocol on a 3.0 T Siemens TrioTim Magnetom system (Erlangen, Germany) using a 32-channel phased-array head coil. T1-weighted magnetization prepared rapid acquisition GRE (MP-RAGE) (TR = 1,850 ms, TE = 4 ms) and high-resolution T2-weighted imaging (TR = 3,200 ms, TE = 380 ms) were performed. Diffusion tensor imaging (DTI) was performed (b values of 300, 700, 2,000 and multiple b = 0 images, single-shot EPI, 50 mm × 2.5 mm axial slices, 96 × 96 matrix zero-filled to 128 × 128, field-of-view 24 cm × 24 cm). Mean diffusivity (MD), radial diffusivity (RD), and fractional anisotropy (FA) were estimated from the diffusion tensor model using the CAMINO toolkit.[5] Tractography was performed with 100,000 seeds in the corpus callosum and white matter generated using an angle threshold of 30° in DSI-Studio using *Q*-space diffeomorphic registration. A NODDI protocol optimized for the scanner (b values of 300, 700, 2,000 and multiple b = 0 images) was obtained. Estimates of neurite density (intracellular volume fraction, ICVF), orientation dispersion index (ODI), and the isotropic fraction (FISO) were obtained from fitting performed with the NODDI Matlab Toolbox.[6]

Third-party tools, ANTs[7] (http://stnava.github.io/ANTs/) and FSL[8] (http://fsl.fmrib.ox.ac.uk/fsl/fslwiki/) framework, were used to register all modalities to the patient's native T1 space. A region of interest (ROI) was manually drawn to include all the SBH on the T1 images because the automated segmentation tools were unable to uniformly segment SBH. Further, the manual ROI was eroded by 1 voxel in all directions to prevent any partial-volume effects from surrounding white matter voxels. In addition, normal-appearing gray and white matter ROIs were segmented using the ANTS segmentation protocol. These ROIs were used to quantify each of the modalities. The same NODDI research protocol and postprocessing were performed on an age-matched healthy female control. Ninety-five age-matched controls with available T1 MP-RAGE were used to compute normal gray and white matter volume.

Results and Discussion

Characteristics of heterotopia on standard structural sequences

T1WI and T2WI (Fig. 1) showed abnormal gray matter (GM) and T2 hyperintensity symmetrically throughout the cerebral cortex, characteristic of SBH. Of total brain volume, 36.3% was normal-appearing gray matter, as determined by automated segmentation, and 6.28% was from heterotopia, as manually outlined, for a total of 42.6% gray matter tissue. The normal-appearing white matter (WM) accounted for 25.1% of all voxels in the patient's cerebrum, and cerebrospinal fluid (CSF) accounted for the remaining 32.3%. Normal healthy controls had 38.5 ± 1.25% gray matter and 30.5 ± 1.09% white matter. Overall, there was slightly more gray matter volume (including heterotopic tissue, z statistic 3.31, $p < 0.001$) and slightly less white matter volume (z statistic –4.96, $p < 0.001$) in the SBH patient. Past histologic observations suggest that the total gray matter neuronal population far exceeds that present in healthy persons, suggesting not just migrational defects but also overproliferation of immature neuronal cell bodies.[9]

MCDs often affect the microstructure of underlying white matter tracts.[10] The presence of heterotopic neurons, abnormal myelination, edema, axonal injury, and gliosis affects the diffusion properties traversing axonal tracts.[10,11] Fig. 1 also shows tractography in the patient (top) and a normal age- and gender-matched control (bottom) obtained by seeding the white matter using DSI-Studio.[12,13] The superior longitudinal fasciculus was not fully rendered in the patient during tractography because of abnormal directional vectors in areas with heterotopic tissue. Other tracts, such as the corpus callosum, cingula, superior occipitofrontal fasciculus, and inferior occipitofrontal fasciculus, were mostly unaffected.

Characteristics of heterotopia on advanced diffusion imaging sequences

It is known histopathologically that subcortical heterotopia has morphologically abnormal neurons in addition to

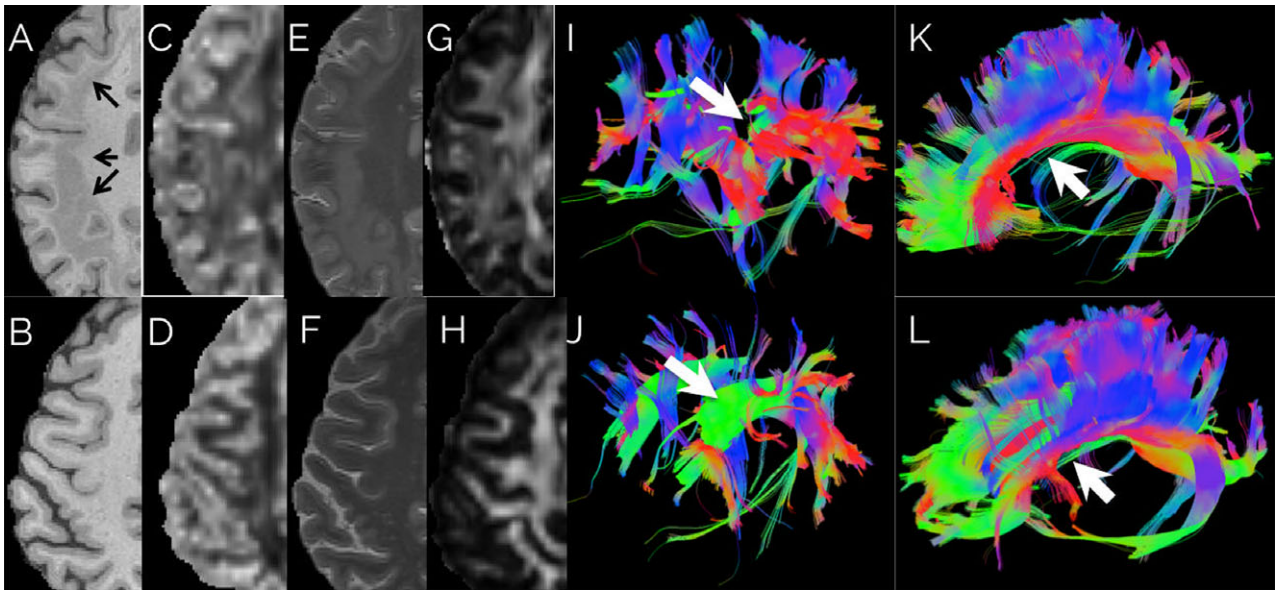

Figure 1.

Patient (top row) and age-matched healthy control (bottom row). (**A**–**H**) First four columns show T1-weighted magnetization prepared rapid acquisition GRE, orientation dispersion index (ODI) derived from NODDI imaging, T2-weighted MRI, and fractional anisotropy, respectively. Band heterotopia (arrows) clearly delineated in a bilateral band located between the ventricular wall and cortical mantle. ODI map shows aberrant neurite dispersion in white matter regions as compared to healthy control ODI map. (**I**–**J**) The fifth column shows tractography obtained by seeding the normal location of the superior longitudinal fasciculus. (**K**–**L**) The sixth column shows tractography obtained by seeding the genu, body, and splenium of the corpus callosum. 3D tract maps are shown in an oblique lateral view, with anterior to the left. The colors represent the direction of the fiber tracts using standard labeling. Most large tracts, such as callosal fibers, could be followed through the heterotopic tissue; however, the superior longitudinal fasciculus (white arrow) was attenuated compared to the control.

demyelinated white matter tracts originating from the cortical plate and the heterotopia.[14] We hypothesized that this alters NODDI and DTI parameters in SBH to be intermediate between GM and WM. Interestingly, although SBH tissue contains neurons and looks like gray matter on structural imaging, it is more similar to white matter on NODDI imaging (Table 1). Using the Kolmogorov–Smirnov goodness of fit hypothesis test, the underlying distribution of NODDI parameters in heterotopia is different from that for gray matter ($D = 0.39$, $p < 0.001$) and white matter ($D = 0.09$, $p < 0.001$). Global neurite dispersion was lower in heterotopia (0.34 ± 0.10) and white matter (0.33 ± 0.14) as compared to gray matter (0.47 ± 0.10). CSF fraction was much less in heterotopia (0.03) and white matter (0.09) as compared to gray matter (0.20). FA was higher in heterotopia tissue (0.29 ± 0.12) and white matter (0.32 ± 0.18) as compared to gray matter (0.14 ± 0.08). However, global neurite density was higher in heterotopia (0.48 ± 0.06) and gray matter (0.46 ± 0.13) as compared to white matter (0.50 ± 0.10). MD and RD values in heterotopic tissue (0.70×10^{-3} and 0.59×10^{-3} mm^2/s, respectively) were similar to surrounding white matter (0.76×10^{-3} and 0.62×10^{-3} mm^2/s, respectively) but less than overlying gray matter (1.0×10^{-3} and 0.96×10^{-3} mm^2/s, respectively). All of the above relationships were also preserved in separate analysis of each cerebral lobe (data not shown). The values of these parameters in the patient's normal-appearing gray

Table 1. Average diffusion parameters in heterotopia, normal-appearing gray and white matter

	FA	ODI	ICVF	FISO
Patient heterotopia	0.28 ± 0.09	0.34 ± 0.09	0.47 ± 0.04	0.02 ± 0.04
Patient (gray matter)	0.14 ± 0.08	0.47 ± 0.10	0.46 ± 0.13	0.20 ± 0.23
Patient (white matter)	0.32 ± 0.17	0.33 ± 0.13	0.50 ± 0.09	0.08 ± 0.12
Control (gray matter)	0.15 ± 0.11	0.46 ± 0.13	0.48 ± 0.14	0.22 ± 0.24
Control (white matter)	0.35 ± 0.19	0.32 ± 0.14	0.55 ± 0.10	0.11 ± 0.15

Average diffusion imaging parameters obtained in the patient and a healthy age-matched control. Fractional anisotropy (FA), NODDI parameters (orientation dispersion index [ODI], neurite density approximated by intracellular volume fraction [ICVF], isotropic volume fraction most likely due to CSF [FISO]).

and white matter were similar to those measured in the healthy control.

Future directions

These diffusion methods have previously shown utility in identifying focal cortical dysplasias (FCDs).[15] Patients with subtle dysplasias showed clear abnormalities on neurite density and neurite dispersion maps, whereas T1WI and T2WI did not necessarily show such clear abnormalities. This case report shows maps of a novel diffusion imaging technique in a patient with band heterotopia. Although this abnormality is visible on standard imaging, NODDI imaging in addition to DTI clearly shows the lesion as well. These results should be investigated by enrolling more patients and carefully studying coregistered imaging and histology data to better characterize tissue alterations that lead to these findings. These advanced diffusion methods can provide additive information to evaluate heterogeneity within SBH that cannot be detected on structural MRI but that may affect clinical presentation. In addition, utilizing this method to image different forms of heterotopia may allow better understanding of structural differences between these malformations. This may further enhance our understanding of the pathophysiologic mechanisms of MCDs.

Acknowledgments

The authors would like to acknowledge Hoameng Ung, Preya Shah, and Peter Hadar for useful discussion on methods and data collection. This study was funded by 1U24-NS-063930 NIH/NINDS The International Epilepsy Electrophysiology Database, P20-NS-080181/P20-NS12006 NIH/NINDS The Epilepsy Bioinformatics Study (EpiBioS), McCabe Pilot Award (University of Pennsylvania), Center for Biomedical Image Computing and Analytics Seed Award (University of Pennsylvania), and the Thornton Foundation. Additional grant funding was provided by NIH 1-T32-NS-091006-01 (Training Program in Neuroengineering and Medicine).

Disclosure

None of the authors has any conflict of interest to disclose. All coauthors have been substantially involved in the study and/or the preparation of the manuscript; no undisclosed groups or persons have had a primary role in the study and/or in manuscript preparation. All coauthors have seen and approved the submitted version of the paper and accept responsibility for its content. We confirm that we have read the Journal's position on issues involved in ethical publication and affirm that this report is consistent with those guidelines.

References

1. Barkovich AJ, Guerrini R, Kuzniecky RI, et al. A developmental and genetic classification for malformations of cortical development: update 2012. *Brain* 2012;135:1348–1369.
2. Jacobs R, Anderson V, Simon Harvey A. Neuropsychological profile of a 9-year-old child with subcortical band heterotopia or "double cortex". *Dev Med Child Neurol* 2007;43:628–633.
3. Janzen L, Sherman E, Langfitt J, et al. Preserved episodic memory in subcortical band heterotopia. *Epilepsia* 2004;45:555–558.
4. Sicca F, Kelemen A, Genton P, et al. Mosaic mutations of the LIS1 gene cause subcortical band heterotopia. *Neurology* 2003;61:1042–1046.
5. Cook PA, Bai Y, Nedjati-Gilani S, et al. Camino: open-source diffusion-MRI reconstruction and processing. *Proc Intl Soc Mag Reson Med* 2006;14:2759.
6. Zhang H, Schneider T, Wheeler-Kingshott CA, et al. NODDI: practical in vivo neurite orientation dispersion and density imaging of the human brain. *NeuroImage* 2012;61:1000–1016.
7. Tustison NJ, Cook PA, Klein A, et al. Large-scale evaluation of ANTs and FreeSurfer cortical thickness measurements. *NeuroImage* 2014;99:166–179.
8. Jenkinson M, Pechaud M, Smith S. BET2: MR-based estimation of brain, skull and scalp surfaces. *Eleventh Annual Meeting of the Organization for Human Brain Mapping*, Toronto, Ontario, Canada. 2005.
9. Mai R, Tassi L, Cossu M, et al. A neuropathological, stereo-EEG, and MRI study of subcortical band heterotopia. *Neurology* 2003;60:1834–1838.
10. Colombo N, Salamon N, Raybaud C, et al. Imaging of malformations of cortical development. *Epileptic Disord* 2009;11:194–205.
11. Shultz SR, O'Brien TJ, Stefanidou M, et al. Neuroimaging the epileptogenic process. *Neurotherapeutics* 2014;11:347–357.
12. Yeh F-C, Wedeen VJ, Tseng W-YI. Generalized q-sampling imaging. *IEEE Trans Med Imaging* 2010;29:1626–1635.
13. Wedeen VJ, Wang RP, Schmahmann JD, et al. Diffusion spectrum magnetic resonance imaging (DSI) tractography of crossing fibers. *NeuroImage* 2008;41:1267–1277.
14. Eriksson SH, Symms MR, Rugg-Gunn FJ, et al. Exploring white matter tracts in band heterotopia using diffusion tractography. *Ann Neurol* 2002;52:327–334.
15. Winston GP, Micallef C, Symms MR, et al. Advanced diffusion imaging sequences could aid assessing patients with focal cortical dysplasia and epilepsy. *Epilepsy Res* 2014;108:336–339.